University of Miskolc
Faculty of Earth and Environmental Sciences and Engineering
Mikoviny Sámuel Doctoral School of Earth Sciences
Head of the doctoral school:
Prof. Dr. Péter Szűcs, professor

Mineralogical-petrological and genetic characterization of Hungarian graphite occurrences with Carpathian outlook

Theses book of Ph.D. dissertation

LÍVIA LESKÓNÉ MAJOROS
Earth Science Engineer

Supervisor:
Dr. Ferenc Kristály
Head of Department, Senior Research Fellow

Institute of Exploration Geosciences
University of Miskolc

Miskolc, 2025

1. Introduction and objective

Natural graphite has been listed as a critical raw material by the European Union since 2011 (Study on the Critical Raw Materials, 2023). Only a few studies dealt with Hungarian graphite occurrences (e.g., Raincsákné Kosáry, 1978; Demény, 1986; Hermesz, 1990), however, modern analytical techniques – such as Raman spectroscopy – allow for more detailed investigations of graphite and graphitized materials.

The aim of my doctoral research was to carry out a comprehensive mineralogical, petrological, and genetic study of graphite occurrences in Hungary. I collected samples from the Uppony Mountains (Dédestapolcsány), the Szendrő Mountains (Szendrőlád, Szendrő, Meszes, Rakacaszend), the Kőszeg Mountains (Velem), and the Sopron Mountains (Fertőrákos). As part of a broader regional comparison within the Carpathian area, I also examined samples from Kokava nad Rimavicou (Slovakia) and Parâng (Southern Carpathians, Romania).

My research focused on the detection of graphite and graphitized material in the samples, the investigation of their crystal structural ordering and genesis, as well as the characterization of the associated mineral parageneses.

During my investigations, I used polarized light microscopy, scanning and transmission electron microscopy, X-ray powder diffraction, X-ray fluorescence spectrometry, trace element geochemistry, thermogravimetry (simultaneous DTA–DT–DTG) and Raman spectroscopy. In addition, I carried out laboratory experiments on graphite enrichment and extraction.

2. The investigated areas and sample collection

The sampling sites are shown in Figure 1. During fieldwork, I collected samples from the Uppony Mountains (Dédestapolcsány), the Szendrő Mountains (Szendrőlád, Szendrő, Meszes, Rakacaszend), the Kőszeg Mountains (Velem), and the Sopron Mountains (Fertőrákos). Sample collection primarily focused on black – potentially graphitic material containing – rocks found in shear zones.

For the broader Carpathian outlook, the graphitic specimen from Kokava nad Rimavicou was obtained from the Mineral Collection of the Ottó Herman Museum in Miskolc (Inv. no. 2017.343; donated by Rudolf Ďuďa). The specimen from the Cătălinul graphite mine (Parâng Mountains, Romania) was provided through the assistance of mining geologist Zoltán Ambrus (Praid/Parajd) and delivered to the Department of Applied Mineralogy at the University of Miskolc.

Figure 1: The sites investigated during my doctoral research (Google Earth)

3. Sample preparation, grinding and separation experiments

During sample preparation, I produced 42 surface-polished and 2 thin sections for optical microscopy (OM), scanning electron microscopy with energy-dispersive X-ray spectroscopy (SEM-EDX) and Raman spectroscopy. Additionally, I powdered samples for X-ray powder diffraction (XRD), transmission electron microscopy (TEM), thermogravimetry (simultaneous DTA-TG-DTG), X-ray fluorescence spectrometry (XRF) and inductively coupled plasma mass spectrometry (ICP-MS). Beyond the sample preparation, I also carried out laboratory experiments on grinding, separation, fractionation and enrichment methods.

4. Applied methods

During my research, I carried out the investigations in the laboratories of the Institute of Exploration Geosciences at the University of Miskolc, using the following equipment:

- Optical examinations:
  - Zeiss Imager.A2m AXIO polarizing microscope, Zeiss AxioCam MRc5 camera
  - Zeiss SteREO Discovery.V20 stereomicroscope, Zeiss AxioCam MRc5 camera
- SEM-EDX:
  - JEOL JXA-8600 Superprobe (20 kV, 20 nA, 60 s)
  - ThermoFisher Helios G4 PFIB CXe (20 kV, 3.2 nA, 50 s) University of Miskolc, 3D labor
  - Phenom ProX (15 kV, 2 mm working distance, low vacuum) University of Miskolc, Institute of Raw Material Preparation and Environmental Technology

- TEM: FEI Tecnai G^2 (University of Miskolc, Institute of Metallurgy, Metal Forming and Nanotechnology)
- XRD:
  - Bruker D8 Advance (Cu K-alfa radiation, 40 kV, 40 mA)
  - Bruker D8 Discover (Cu K-alfa radiation, 40 kV, 40 mA)
- XRF: Rigaku SuperMini200 WDS (LiF200 / PET / XR25 crystals, Pd cathode, 200 W, 50 kV, 4 mA)
- ICP-MS: ALS Global
- Simultaneous DTA-TG-DTG: MOM Derivatograph-C (10 °C/min, linear heating, air, corundum crucible) University of Miskolc, Institute of Energy and Quality
- Raman spectroscopy: Thermo Scientific DXR (532 nm (green) laser, 2 mW, 3×15 s exp. time, ~4 cm^{-1} spectral resolution – FWHM, 100X objective, 50 μm pinhole aperture) University of Szeged, Department of Geology

5. Results

Based on the OM and SEM-EDX measurements, the matrix of the samples was quartz in the Dédestapolcsány and Kokava nad Rimavicou samples (Majoros, 2019); calcite and muscovite in the Szendrőlád samples (Majoros et al., 2022); quartz and phyllosilicates (muscovite, chlorite) in the samples from Szendrő, Meszes (Leskóné Majoros et al., 2021), Rakacaszend, Velem and Fertőrákos (Leskóné Majoros et al., 2025a); while muscovite in the samples from Parâng (Majoros, 2019).

As for the main accessory minerals, the samples contained TiO_2 (rutile and anatase based on optical observations), zircon, monazite-(Ce) grains, xenotime, allanite, fluorapatite, goyazite–gorceixite solid solution series, bastnäsite–parisite-(Ce) series, bastnäsite-(Ce) and bastnäsite-(La) solid solutions and graphite.

During the TEM measurements, in all cases, I examined the fractions obtained during the enrichment experiments of the samples using preparations made on Cu grids. In the Parâng sample, as well as in the "silver-grey" fraction of the Dédestapolcsány sample, I observed 400–800 nm sized idiomorphic to hypidiomorphic graphite grains with hexagonal shape and well-ordered crystal structure. In contrast, the "black" fraction of the Dédestapolcsány sample contained idiomorphic to hypidiomorphic grains of 400–600 nm in size, with (pseudo-) hexagonal shape and partial structural ordering. In the Szendrőlád sample, I identified graphite grains measuring 80–200 nm in size with an ordered crystal structure, whose appearance corresponds to hexagonal dipyramidal graphite in a c-axis view (Palache et al., 1944).

In the case of the Hungarian samples, graphite could not be clearly identified by XRD analysis due to the significant

overlap between graphite and quartz reflections. The main graphite peak between 26°–27°(2θ) (hkl = 002) nearly coincides with the quartz peak, resulting in an asymmetric composite peak. The other graphite peaks do not appear in the diffractograms due to the low graphite content and preferred orientation. However, with Rietveld refinement, the presence of graphite in the Hungarian samples could be confirmed.

In contrast, for the museum specimen from Kokava nad Rimavicou and the sample from Parâng, the presence of graphite was evident even in the XRD analysis, and both polytypes could be observed as well (Majoros, 2019).

Although graphite cannot be detected directly by XRF analysis, I still performed such measurements in order to complement and support the results of the SEM-EDX and XRD analyses by determining the major and trace element contents of the samples. Except for the museum specimen from Kokava nad Rimavicou and the samples from Szendrő, I powdered and examined samples from all localities using the XRF method.

The major and trace element contents determined by XRF are consistent with the findings of the SEM-EDX and XRD analyses. Furthermore, the XRF analysis also allows for semi-quantitative evaluation of the measured samples. Among the data, the high vanadium content (~200–700 ppm) of the samples from Dédestapolcsány, Szendrőlád, Velem, Fertőrákos, and Parâng stands out, which is in accordance with the observations made during the SEM-EDX and XRD analyses.

Figure 2 shows the trace element compositions obtained from the ICP-MS analyses, normalized to PAAS (values after Taylor and McLennan, 1985). Among the results, notably high contents were observed for V (in the Dédestapolcsány and Szendrőlád drill core samples), Sm (in the Szendrőlád drill core and Szendrő samples), Sr (in the Szendrőlád samples), U (in the

Dédestapolcsány and Szendrőlád drill core samples), Nb (in the Szendrőlád drill core samples), and Ba (in the Dédestapolcsány samples). A negative anomaly was observed for Rb and Th in all samples.

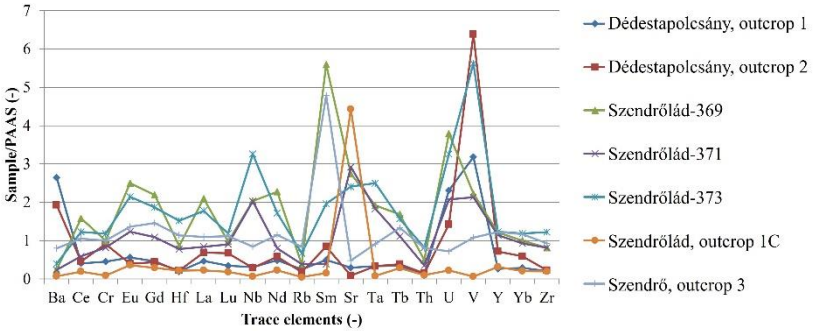

Figure 2: Results of trace element contents normalized to PAAS obtained during ICP-MS analysis (PAAS values after Taylor and McLennan, 1985)

During the simultaneous DTA-TG-DTG analyses, the exothermic reaction of graphite was observed in all samples at temperatures around ~600–800 °C. In addition to the thermal reaction of graphite, an exothermic reaction of organic matter (partially graphitized material) was also detected between ~150–500 °C in the samples from Dédestapolcsány (Figure 3), Szendrőlád and Szendrő.

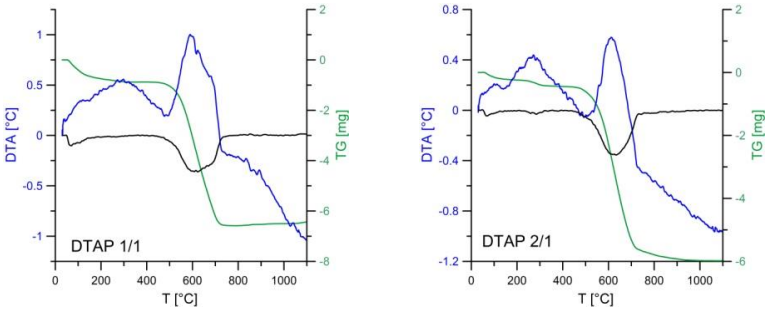

Figure 3: Results of simultaneous DTA-TG-DTG analysis (blue – DTA, green – TG, black – DTG), Dédestapolcsány

During the Raman spectroscopy measurements, in addition to the G band (~1580 cm^{-1}), D-bands also appeared in my samples (D1 band at ~1350 cm^{-1} & D2 band at ~1620 cm^{-1}) in the first-order region. In the second-order region, three bands (S2, S3 & S4) were identifiable in the Dédestapolcsány sample, while four bands were observed in the other samples: three bands (S1, S3 & S4) appeared with low intensity, and one band (S2) with high intensity. Figure 4 shows an evaluated Raman spectrum, displaying the first- and second-order graphite bands.

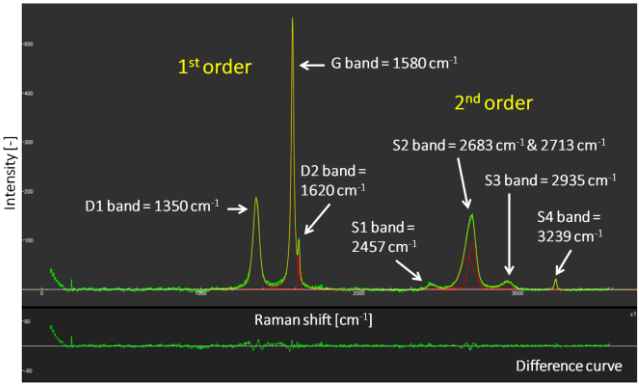

Figure 4: An evaluated Raman spectrum, displaying the first- and second-order graphite bands. Fertőrákos (Leskóné Majoros et al., 2025a)

6. Discussion

6.1. Detection of graphite

SEM-EDX analyses revealed the presence of a carbonaceous material in all samples – except for the Szendrőlád samples collected from the outcrops at Helle Creek – which was confirmed by optical observations that were graphitized. In almost all cases, the graphitized material was characterized by undulose extinction, bireflectance and anisotropic behavior.

By XRD analysis, graphite could not be identified in the case of Hungarian samples; however, its presence could be confirmed through Rietveld refinement.

Simultaneous DTA-TG-DTG analysis also proved suitable for detecting and quantifying the graphite and organic matter content of the samples, though this method does not provide information on the crystal structural ordering of graphite. For this purpose, Raman spectroscopy and TEM offered appropriate solutions. The thermogravimetric analyses confirmed the presence of graphite in all cases, while TEM measurements provided insight into the lattice structure and degree of ordering of individual graphite grains.

6.2. Genetic relations of graphite crystallization

Using the Raman spectrum of graphite, it is suitable for determining the peak formation temperature (Henry et al., 2019). First, I used the formula of Beyssac et al. (2002) and then the formula of Aoya et al. (2010) to calculate the peak formation temperature. The obtained temperature values fit into the geological background of the studied areas (Fülöp, 1994; Babinszki et al., 2024; Ion et al., 2023).

At all studied localities, the graphite is formed syngenetically during regional metamorphism; shear-related deformation facilitated the progressive transformation of organic matter into graphite (i.e. graphitization) within the host rocks.

The graphite occurrences I have examined genetically fit into the category of type 4B – metamorphosed graphite deposits (Kužvart, 1984). The Hungarian and Kokava nad Rimavicou occurrences fall into the subcategory of graphite deposits formed during regional metamorphism, while the Parâng occurrence falls into the subcategory of graphite deposits formed during regional and then contact metamorphism.

6.3. Economic geological assessment

For the economic geological evaluation of graphite, it is necessary to consider its grain size (important for application point of view), its quantity in the rocks and its extractability.

According to the raw material trade classification (Mitchell, 1993), the graphite in the samples can be classified into two categories: "amorphous" (cryptocrystalline, grains <70 μm) and "flaky graphite" (fine-grained 70–150 μm and coarse-grained >150 μm flakes).

Regarding the quantity of graphite, it can be inferred from the thermogravimetry analyses and the graphite contents calculated by Rietveld refinement. The combined use of these methods gives a good estimate of the amount of organic and graphitized material in the samples (Majoros et al., 2022).

Regarding the Hungarian samples, the amount of graphite and graphitized material was everywhere ~2–5 wt%. However, by exploiting the hydrophobic nature of graphite, it was possible to enrich the samples to a graphite content of ~10 wt%.

7. Scientific theses

1. **New results related to X-ray powder diffraction examinations:**
   a) **I found that during the X-ray powder diffraction examination of the bulk rock of the Hungarian potentially graphite-containing samples I examined, it is not possible to clearly detect graphite (due to overlapping peaks, preferred orientation and small amount). Rietveld refinement is required to determine the graphite content, but cannot be solved without optical microscopy and Raman spectroscopy, as well as thermogravimetry.**

In most cases, using Rietveld refinement, it is only possible to quantitatively calculate the graphite content in the samples, if its presence has been proven at least by optical microscopy and Raman spectroscopy methods (Figure 5). However, it is still necessary to check and correct the obtained results with thermogravimetry, due to the high possibility of error.

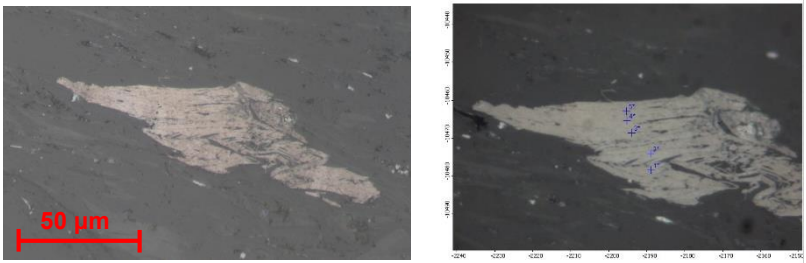

Figure 5: Graphite flake under polarizing microscope, reflected light, examined at 1N (left), and the location of Raman spectroscopy measurements within the graphite flake (right). Meszes

b) **During Rietveld refinement, while in a simple matrix like calcite (no peak overlapping) detection limit of the graphite content can be approximately 0.5 wt%, in quartz matrix this value is ~1 wt%. In contrast, in a more complex sample containing both phyllosilicates and quartz, the detection limit of graphite might be even ~5 wt% (Leskóné Majoros et al., 2025b).**

Visual confirmation is therefore necessary before XRD evaluation, as the deconvolution procedures of the Rietveld refinement allow the calculation of the amount of each phase even in the case of peak overlap and 1–5 wt% amounts, provided that the given phase is actually present in the sample (Leskóné Majoros et al., 2025b).

2. **Based on the Raman spectroscopy results, I determined the average peak formation temperature of graphite by graphite geothermometry using the formulas of Beyssac et al. (2002) and Aoya et al. (2010). The calculated average formation temperature:**
   a) **from the Uppony Mts. area (Dédestapolcsány, Rágyincs Valley): ~335 °C (±50 °C),**
   b) **from the Szendrő Mts. area (Szendrőlád and Meszes): ~405 °C (±50 °C) (Majoros et al., 2022) and ~420 °C (±50 °C) (Leskóné Majoros et al., 2025b),**
   c) **from the Kőszeg Mts. area (Velem): ~400 °C (±50 °C),**
   d) **from the Sopron Mts. area (Fertőrákos): ~440 °C (±50 °C) (Leskóné Majoros et al., 2025a).**

Using the Raman spectrum of graphite, it is suitable for determining the peak formation temperature (Henry et al., 2019). One of the parameters required for this is the R2 area ratio value, which can be calculated based on the following equation:

$$R2 = D1 / (G + D1 + D2),$$

where G = G band area, D1 = D1 band area, D2 = D2 band area.

First, I used the formula of Beyssac et al. (2002) to calculate the peak formation temperature:

$$T\ (°C) = -445*R2 + 641\ (\pm 50\ °C).$$

This equation gives the maximum temperature between 330 and 650 °C. Although the equation is developed for graphite formed during regional metamorphism, it is done using a 514.5 nm laser. However, my measurements were made with a 532 nm laser, so I looked for another equation that also uses a 532 nm laser.

Thus, I also applied the formula of Aoya et al. (2010):

$T\ (°C) = 221*(R2)^2 - 637{,}1*R2 + 672{,}3\ (\pm 50\ °C)$.

The latter equation is valid between 340 and 655 °C and was developed for contact metamorphic rocks. Considering the measurement conditions (use of lasers with different wavelengths) and the rocks that have undergone different metamorphisms, any equation can be used, based on the findings of Aoya et al. (2010), since the difference calculated for the peak formation temperature is in all cases less than 10 °C (according to their measurements, it falls between 5–10 °C), which is well within the error range (±50 °C).

Table 1 contains the R2 values, and the formation temperature results calculated using the two formulas for each locality.

Table 1: The obtained average peak formation temperature results (±50 °C) using the two formulas and the difference between the calculated temperature values for each locality

	R2 value [-]	**Temperature based on Beyssac et al. (2002) [°C]**	**Temperature based on Aoya et al. (2010) [°C]**	**Difference [°C]**
Dédestapolcsány	0.69	334	338	-4
Szendrőlád, SZL-6	0.53	408	400	8
Meszes	0.48	425	417	8
Velem	0.54	401	394	7
Fertőrákos	0.44	443	434	9
Parâng	0.56	390	384	6

3. **My findings related to the morphology of graphite:**
   a) **Based on the morphology and textural characteristics of graphite, I defined two basic types in the Hungarian samples:**
      - **Flaky appearance: rock-coloring flakes (1–20 μm in size, scattered in the matrix, Dédestapolcsány), non-deformed flakes (20–100 μm in size, e.g. Dédestapolcsány, Szendrőlád, Meszes, Velem, Fertőrákos), and deformed flakes (kink-band microstructure, 20–150 μm in size, e.g. Szendrő, Meszes, Rakacaszend).**
      - **Aggregate appearance: granular aggregate (10–30 μm in size in Meszes and 50–300 μm in Fertőrákos), aggregate (graphitic mixture, 30–300 μm in size, for example graphite-sericite-quartz at Dédestapolcsány, graphite-muscovite-calcite or graphite-Ti-Zr mixture at Szendrőlád), and microfold, lenticular aggregate (flakes with a size of 20–50 μm are arranged into plate-like aggregates with a size of >300 μm, forming microfolds, e.g. Szendrőlád).**

In samples from different sites, graphite was observed with different morphology (Figure 6), size and order structure (sometimes even within a single sample). This mainly depends on the amount and distribution of available organic matter in the rock, as well as the deformation (shear) effects that cause graphitization (Buseck and Beyssac, 2014).

Based on morphology, six groups could be distinguished which can be classified into two main basic types: flaky appearance (1–3.) and aggregate appearance (4–6.):

1. Rock-coloring flakes (1–20 μm in size, scattered in the matrix, e.g. Dédestapolcsány and Parâng)
2. Non-deformed flakes (20–100 μm in size, for example at Dédestapolcsány, Szendrőlád, Meszes, Velem, Fertőrákos, and 100–1000 μm in size at Kokava nad Rimavicou)
3. Deformed flakes (kink-band microstructure, 20–150 μm in size, e.g. Szendrő, Meszes, Rakacaszend, and 100–800 μm in size at Parâng)
4. Granular aggregate (10–30 μm in size in Meszes and 50–300 μm in Fertőrákos)
5. Aggregate (graphitic mixture, 30–300 μm in size, for example graphite-sericite-quartz at Dédestapolcsány, graphite-muscovite-calcite or graphite-Ti-Zr mixture at Szendrőlád)
6. Microfold, lenticular aggregate (flakes 20–50 μm in size are arranged into plate-like aggregates >300 μm in size, forming microfolds, e.g. Szendrőlád)

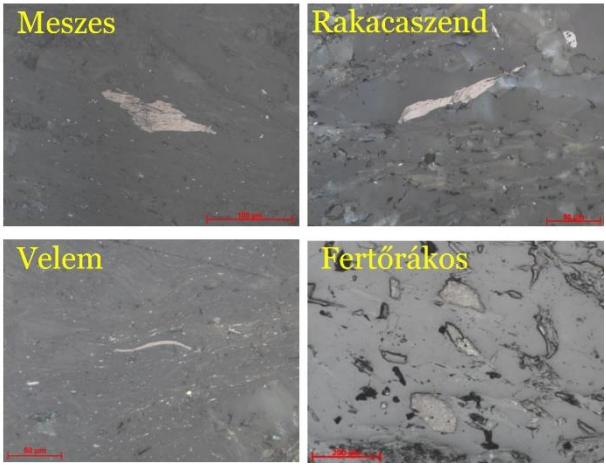

Figure 6: Different morphologies of graphite flakes and aggregates, polarizing microscope, reflected light, 1N

b) I found and described for the first time graphite with hexagonal dipyramidal morphology from a Hungarian site (Szendrőlád, Helle Creek, Szendrő Mountains).

During the TEM examinations, I identified 80–200 nm sized graphite grains with ordered crystal structure in the Szendrőlád sample, whose appearance corresponds to hexagonal dipyramidal graphite in the c-axis view (Figure 7) (Palache et al., 1944).

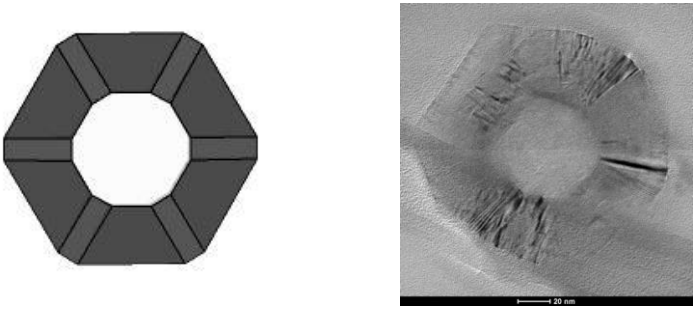

Figure 7: Graphite grain with hexagonal dipyramidal appearance and ordered crystal structure in c-axis view (theoretical model[1] – left, Szendrőlád sample – right)

[1]Theoretical model: https://www.mindat.org/min-1740.html. Last updated: 29.03.2025

4. **For the Hungarian samples, I determined that graphite have formed syngenetically with metamorphism, developing within shear zones during regional metamorphic processes.**

The texture of the samples well reflects the oriented texture formed as a result of deformation, in which the deformation related elements characteristic for shear zones were also clearly observed: crenulation cleavage, microfolds (Figure 8), deformation twinning of calcite crystals, strain shadows around rutile grains and undulose extinction of graphite flakes.

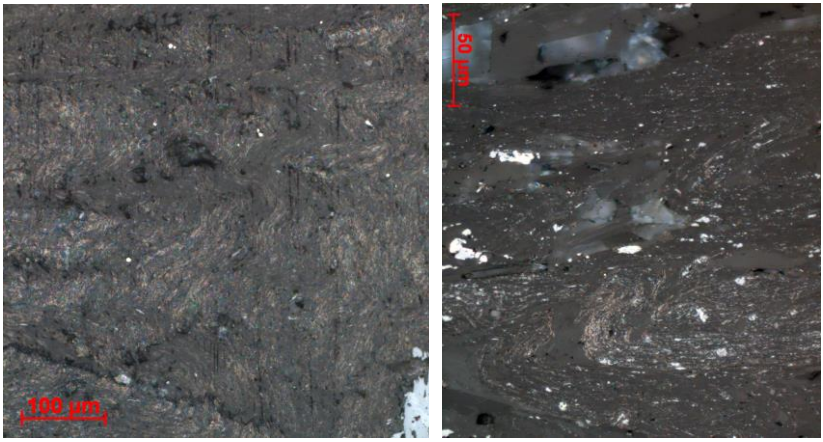

Figure 8: Oriented graphite flakes forming microfolds (light brown). Polarizing microscope, reflected light, 1N. Szendrőlád (Majoros, 2019)

5. **My findings regarding the crystal structure order of graphite:**

   a) **I ranked the Hungarian formations based on the crystallinity degree R1 (R1=D1/G intensity ratio) and G_{FWHM} (G-band full width at half maximum) of the graphitized material found in them. Showing the order of the crystal structure from the smallest to the largest, I have established the following order:**
      - **Tapolcsány Formation (R1=4,34 & G_{FWHM}=126)**
      - **Szendrőlád Limestone Formation (R1=0,94 & G_{FWHM}=30)**
      - **Kőszeg Metamorphic Complex (R1=0,77 & G_{FWHM}=22)**
      - **Szendrő Phyllite Formation (R1=0,57 & G_{FWHM}=21)**
      - **Fertőrákos Metamorphic Complex (R1=0,44 & G_{FWHM}=20)**

b) Based on the formation temperature values calculated with graphite geothermometry and the DTA peak temperature results obtained during thermogravimetric analysis, I have determined that the more ordered the crystal lattice of the graphite found in the Hungarian samples, the higher its oxidation temperature (Figure 9)**.**

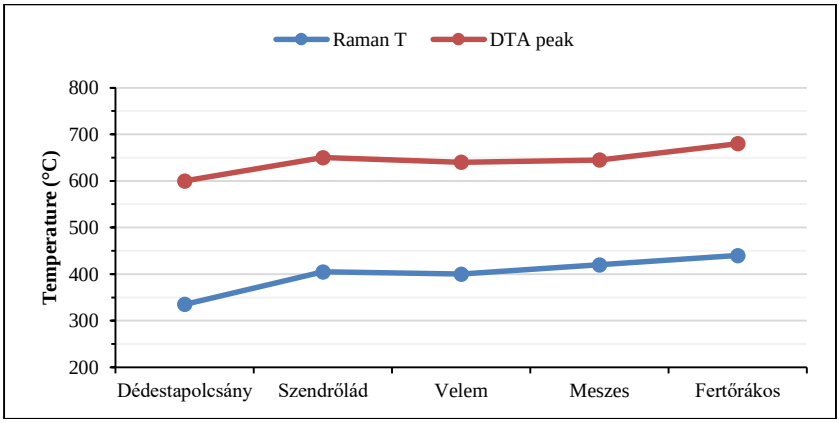

Figure 9: Line diagram of the formation temperature values calculated with graphite geothermometry and the DTA peak temperature results obtained during thermogravimetric analysis

6. **I determined that among the minerals carrying critical elements associated with graphite, the enrichment of TiO_2 phases (>1 wt%) and as a substitute element, V is significant (~200–1000 ppm) in the examined samples. By interpreting the trace element content, I observed the following geochemical trends:**
    - **The V content is exceptionally high in the Dédestapolcsány, Szendrőlád, Parâng and Kokava nad Rimavicou samples** (Table 2)**. In the latter, this causes the macroscopically seen light green color of muscovites (**Figure 10**; Majoros, 2019).**

Table 2: V content of the samples based on ICP-MS analysis (ppm). The V content of Parâng sample is based on semi-quantitative analysis of XRF method (ppm). PAAS values after Taylor and McLennan (1985)

	PAAS	Dédestap. outcrop 1.	Dédestap. outcrop 2.	Szendrőlád 369	Szendrőlád 371	Szendrőlád 373	Parâng
V	150	477	957	334	320	843	473

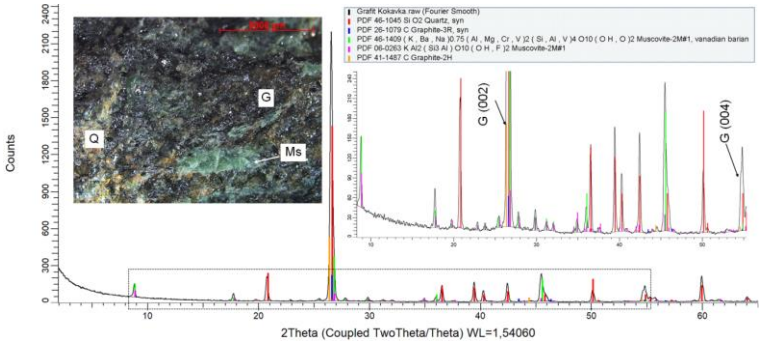

Figure 10: Diffractogram of the museum specimen from Kokava nad Rimavicou. The measured surface is in the middle left, and the framed part is enlarged in the middle right (Majoros, 2019)

- **The high vanadium content in the samples is not accompanied by significant chromium enrichment. Although I did not identify any Cr-containing phase during the SEM-EDX measurements, I observed that the Cr content of the samples shows a similar trend to the V content** (Figure 11)**.**

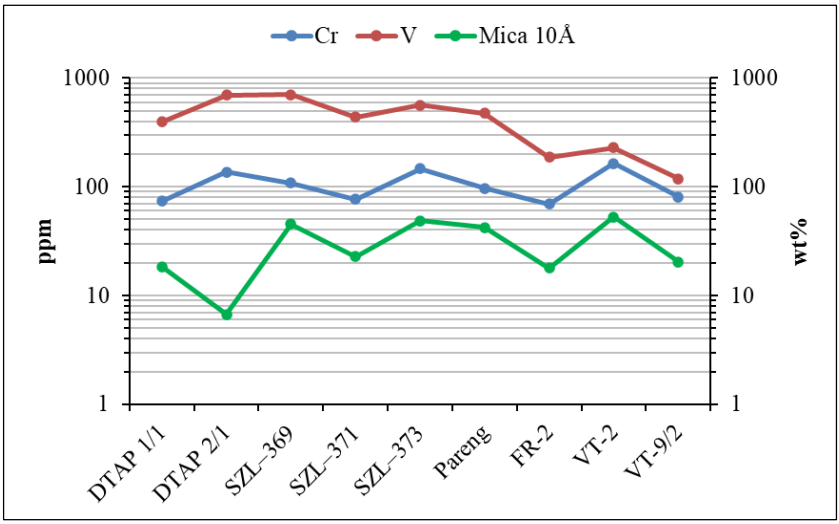

Figure 11: The Cr and V content (ppm) of the samples based on XRF measurement, and the 10Å mica content (wt%) determined during Rietveld refinement plotted on a logarithmic scale

7. **New mineral description from a Hungarian site:**
   a) **I was the first to describe solid solution series of goyazit-gorceixite composition from the Dédestapolcsány samples (Uppony Mountains) (Majoros, 2017).**
   b) **I was the first to describe molybdenite mineral, as well as bastnäsite-(Ce) and bastnäsite-(La) solid solution series in the Szendrő Mts. (Szendrőlád – Majoros et al., 2022).**
   c) **I was the first to describe allanite mineral, as well as bastnäsite-(Ce) and bastnäsite-(La) solid solution series from the Velem samples (Kőszeg Mountains,** Figure 12**). Previously, Demény (1986) detected apatite from this area by optical microscopy, but during my SEM-EDX measurements I was able to clarify that all apatite is fluorapatite.**

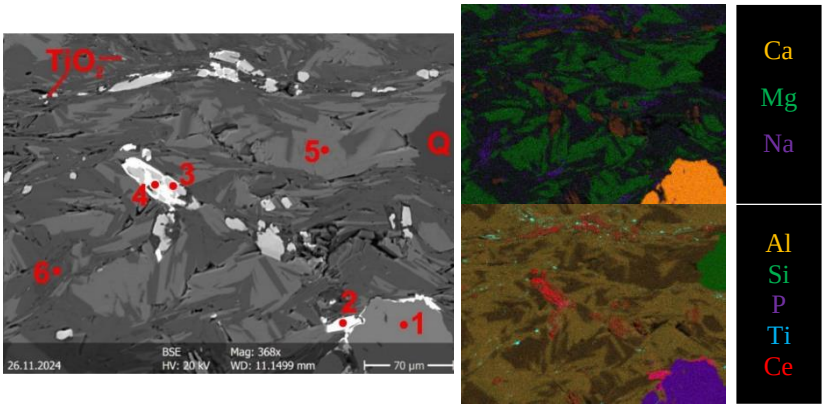

Figure 12: Apatite (1st point) with monazite in the marginal part (2nd point), as well as allanite grains (3rd point) next to bastnäsite solid solutions series (4th point) in the mica matrix (chlorite – 5th point and Na-bearing muscovite – 6th point), scattered with TiO_2 grains and quartz (Q). BSE image (left), SEM-EDX element maps (right). Velem

8. **I carried out the raw material trade classification of graphite found in Hungarian samples based on Mitchell (1993). I was able to classify the graphite grains detected in the samples into the following categories:**
    - **"Amorphous" (cryptocrystalline, grains <70 µm): 1–20 µm, rock-coloring flake graphite scattered in the matrix of the Dédestapolcsány samples (Majoros, 2019); 20–50 µm flakes observed in the Szendrőlád samples (Majoros et al., 2022); 10–50 µm flakes in the Meszes (Leskóné Majoros et al., 2021), Velem and Fertőrákos (Leskóné Majoros et al., 2025a) samples.**
    - **"Flaky graphite" (fine-grained 70–150 µm and coarse-grained >150 µm flakes): graphite flakes >70 µm detected in samples from Dédestapolcsány, Szendrő, Meszes (Leskóné Majoros et al., 2021), Rakacaszend and Fertőrákos (Leskóné Majoros et al., 2025a).**

9. I performed a graphite enrichment experiment for the examined Hungarian occurrences. The experiment was successful; I was able to enrich the graphite content in the samples by an average of 3–5 times by exploiting the hydrophobic nature of graphite.

Regarding the Hungarian samples, the amount of graphite and graphitized material was everywhere ~2–5 wt%. However, by exploiting the hydrophobic nature of graphite, it was possible to enrich the samples to a graphite content of ~10 wt% (Table 3).

Table 3: Summary table of the original graphite content in the samples (calculated by Rietveld refinement), the graphite content of the fraction extracted during the enrichment experiment (calculated by Rietveld refinement) and the enrichment factor

Sample	Original graphite content [wt%]	Extracted fraction [wt%]	Enrichment factor [-]
DTAP 2/1	2,1	10,1	4,8
SZL-1A	2,2	10,3	4,7
M-3B	2,7	7,9	2,9
VT-9/2	0,3	8,3	33,2
FR-2	5,7	7,6	1,3

8. References in the theses book

Aoya M., Kouketsu Y., Endo S., Shimizu H., Mizukami T., Nakamura D. and Wallis S. (2010): Extending the applicability of the Raman carbonaceous material geothermometer using data from contact metamorphic rocks. Journal of Metamorphic Geology, 28, 895–914.

Babinszki E., Piros O., Budai T., Gyalog L., Halász A., Király E., Koroknai B., Lukács R. and M. Tóth T. (eds.) (2024): Lithostratigraphic units of Hungary I. Pre-Cenozoic formations. Supervisory Authority for Regulatory Affairs, Budapest, 276 p.

Beyssac O., Goffé B., Chopin C. and Rouzaud J. N. (2002): Raman spectra of carbonaceous material in metasediments: a new geothermometer. Journal of Metamorphic Geology, 20, 859–871.

Buseck P. R. and Beyssac O. (2014): From organic matter to graphite: Graphitization. Elements, 10, 421–426.

Demény A. (1986): Petrological-geochemical investigation of the parametamorphites of the Kőszeg Mountains (in Hungarian). Thesis, ELTE, Department of Petrology and Geochemistry, Budapest.

Fülöp J. (1994): Geology of Hungary, Paleozoic II. (in Hungarian). Akadémiai Kiadó, Budapest, 9–118.

Henry D. G., Jarvis I., Gillmore G. and Stephenson M. (2019): Raman spectroscopy as a tool to determine the thermal maturity of organic matter: Application to sedimentary, metamorphic and structural geology. Earth-Science Reviews, 198, 102936, pp. 19.

Hermesz M. (ed.) (1990): Geological and geophysical analysis of graphite bearing occurrences in the Szendrő Mts. (in Hungarian). TIT, Environmental Protection and Technical

Service Working Group of Nógrád County, Unpublished report, National Geological and Geophysical Repository, Budapest, 200 p.

Ion A., Cosac A. and Ene V. V. (2023): Natural radioactivity level in graphite samples from the Cătălinul deposit, Parâng Mountains, Romania: sources identification and radiological risk assessment. Review of the Bulgarian Geological Society, 84 (3), 245–248.

Kužvart M. (1984): Industrial minerals and rocks. Elsevier, Prague, 18, 454 p.

Leskóné Majoros L., Leskó M. Zs., Szakáll S. and Kristály F. (2021): Critical minerals and elements in the Szendrő Phyllite Formation (Szendrő Mts., NE-Hungary) (in Hungarian). Multidisciplinary Sciences, 11 (1), 90–97.

Leskóné Majoros L., Leskó M. Zs., Fintor K., Bulátkó-Debus D., Móricz F., Szakáll S. and Kristály F. (2025a): Analyses of graphite-bearing schists from Fertőrákos, Sopron Mts., NW-Hungary. Geosciences and Engineering, 12 (2), 86–97.

Leskóné Majoros L., Leskó M. Zs., Fintor K., Móricz F., Bulátkó-Debus D., Szakáll S. and Kristály F. (2025b): Accessory graphite in phyllites as indicator of metamorphic grade and stage (Szendrő Mts., NE-Hungary). Geosystems and Geoenvironment, 4, 100431.

Majoros L. (2017): Mineralogical characterization and genetics of graphite from Dédestapolcsány (in Hungarian). TDK thesis, University of Miskolc, Institute of Mineralogy and Geology, Miskolc.

Majoros L. (2019): Mineralogical and petrographical examinations of graphitic materials in black schists from Uppony Mts and Szendrő Mts and their Carpathian connections (in Hungarian). University of Miskolc, Institute of Mineralogy and Geology, MSc diploma thesis, 102 p.

Majoros L., Fintor K., Koós T., Szakáll S. and Kristály F. (2022): Metamorphic graphite from Szendrőlád (Szendrő Mts., NE-Hungary) detected by simultaneous DTA-TG. Journal of Thermal Analysis and Calorimetry, 147, 3417–3425.
Mitchell C. J. (1993): Industrial Minerals Laboratory Manual: Flake Graphite. BGS Technical Report, Keyworth, Nottingham, WG/92/30.
Palache C., Berman H. and Frondel C. (1944): The system of mineralogy. Vol I, 7th edition, John Wiley & Sons, New York.
Raincsákné Kosáry Zs. (1978): Devonian formations of the Szendrő Mountains (in Hungarian). Geologica Hungarica, Series Geologica, 18, 1–113.
Study on the Critical Raw Materials for the EU 2023. Final Report. European Comission. doi: 10.2873/725585.
Taylor S. R. and McLennan S. M. (1985): The Continental Crust: Its Composition and Evolution. Blackwell, Oxford, UK.

9. Publications published on the research topic

Scientific journal articles

Leskóné Majoros L., Leskó M. Zs., Szakáll S. and Kristály F. (2021): *Critical minerals and elements in the Szendrő Phyllite Formation (Szendrő Mts., NE-Hungary) (in Hungarian).* Multidisciplinary Sciences, 11 (1), 90–97.

Majoros L., Fintor K., Koós T., Szakáll S. and Kristály F. (2022): *Metamorphic graphite from Szendrőlád (Szendrő Mts., NE-Hungary) detected by simultaneous DTA-TG,* Journal of Thermal Analysis and Calorimetry, 147, 3417–3425.

Leskóné Majoros L., Leskó M. Zs., Fintor K., Bulátkó-Debus D., Móricz F., Szakáll S. and Kristály F. (2025a): *Analyses of graphite-bearing schists from Fertőrákos, Sopron Mts., NW-Hungary,* Geosciences and Engineering, 12 (2), 86–97.

Leskóné Majoros L., Leskó M. Zs., Fintor K., Móricz F., Bulátkó-Debus D., Szakáll S. and Kristály F. (2025b): *Accessory graphite in phyllites as indicator of metamorphic grade and stage (Szendrő Mts., NE-Hungary),* Geosystems and Geoenvironment, 4, 100431.

Other conference publications

Majoros L., Kristály F. and Szakáll S. (2018): *Graphite in black schists from Dédestapolcsány (Uppony Mts.), Gadna and Szendrőlád (Szendrő Mts.) in NE-Hungary.* Joint 5th Central-European Mineralogical Conference and 7th Mineral Sciences in the Carpathians Conference, Banská Štiavnica, Slovakia, Book of abstracts, p. 69.

Majoros L., Kristály F. and Fintor K. (2019): *Origin of graphite in black schists from Szendrő Mts (NE-Hungary).* 1st International Student Conference on Geochemistry and Mineral Deposits, Prague, Czech Republic, Book of abstracts, 33–34.

Majoros L., Kristály F. and Szakáll S. (2019): *Investigation of potentially graphite-bearing black schists in NE-Hungary (in Hungarian).* Műszaki Földtudományi Közlemények, 88 (2), 134–139.

Majoros L. and Kristály F. (2020): *Mineralogical characterization of graphitic materials in black schists from Szendrő Mts (NE-Hungary).* Doctoral Students Forum Section Publication, University of Miskolc, Faculty of Earth Sciences and Engineering, 29–42.

Leskóné Majoros L., Karacs G., Koós T. L., Szakáll S. and Kristály F. (2021): *Critical minerals in black schists from Szendrőlád (Szendrő Mts., NE-Hungary),* Acta Mineralogica-Petrographica, Abstract Series, Szeged, Vol. 11, p. 26.

Leskóné Majoros L., Szakáll S. and Kristály F. (2022): *Critical elements from the Tapolcsány Formation (Uppony Mts., NE-*

Hungary). In: Christie, A. B. (ed.): Proceedings of the 16th SGA Biennial Meeting: The critical role of minerals in the carbon-neutral future. Rotorua, New Zeeland: Society for Geology Applied to Mineral Deposits, p. 105.

Leskóné Majoros L., Szakáll S. and Kristály F. (2022): *Comparison of critical mineral and element content of black schists from NE-Hungary.* In: Fouillard G., Farhat M., Haider U. and Boddy M. (eds.): 13th Annual PDAC-SEG Student Minerals Colloquium – Abstracts, 41–42.

Leskóné Majoros L., Leskó M. Zs., Fintor K., Szakáll S. and Kristály F. (2022): *Graphite crystallization in shear zones (Szendrő Mts., NE-Hungary).* In: 23rd Meeting of the International Mineralogical Association (IMA 2022): Abstracts, p. 444.

Leskóné Majoros L., Szakáll S. and Kristály F. (2022): *Analysis of critical elements from the Tapolcsány Formation (NE-Hungary).* In: Fehér B., Molnár K., Lukács R., Czuppon Gy. and Kereskényi E. (eds.): Calce et malleo – With lime and hammer: 12th Petrological and Geochemical Wandering Assembly. Budapest, Astronomy and Earth Science Research Center, 89–92.

Leskóné Majoros L., Leskó M. Zs., Fintor K., Szakáll S. and Kristály F. (2022): *Graphite Occurrences in NE-Hungary.* In: Szabó N. P. and Virág Z. (eds.): New results in Earth and Environmental Sciences and Engineering 2022. University of Miskolc, Faculty of Earth and Environmental Sciences and Engineering, 49–56.